Discussion of the flicker noise origin at very low temperature and polarisation operation

Dimitri Boudier and Bogdan Cretu
ENSICAEN, UNICAEN, CNRS, GREYC
University of Caen
Caen, France
bogdan.cretu@ensicaen.fr

Eddy Simoen and Anabela Veloso
Imec
Leuven, Belgium
eddy.simoen@imec.be

Cor Claeys
ESAT-INSYS
KU Leuven
Leuven, Belgium
cor.claeys@kuleuven.be

***Abstract*— Low frequency noise measurements are performed at very low temperature (i.e. 10 K) and for applied drain and gate voltages leading to step-like behaviors in the drain current transfer characteristics. It is shown that for the investigated low applied biases, the Coulomb scattering explains the 1/*f* behavior versus the applied voltages.**

Keywords—Flicker noise, number fluctuations, mobility fluctuation, Coulomb scattering, very low polarization, cryogenic temperature

I. INTRODUCTION

Several studies at cryogenic temperatures concerning n-channel gate all around (GAA) nanowire (NW) FETs have been already reported (e.g. [1]). Moreover, in [2], a novel approach leading to a new theoretical formulation valid in moderate inversion for temperatures (T) lowe than 40 K has been constructed for the mobility fluctuations ($\delta\mu$) and for the carrier number with correlated mobility fluctuations ($\delta n+\delta\mu$) models. These models takeinto account the mobility law that governs the carrier transport for T < 40 K, i.e., the Coulomb scattering at low vertical fields and surface roughness scattering at high vertical fields [3,4].

In this work, additional low frequency noise measurements are analyzed in order to have information on the flicker noise origin at very low applied biases and temperature operation.

An extension of the model of [2] is constructed, given a novel improved theoretical formulation valid also in weak inversion. This extended model may be applied when low frequency noise measurements are performed at fixed drain voltage without any additional considerations.

It is demonstrated that for the investigated applied biases, even if a step-like behavior is present in the drain current characteristics, the Coulomb scattering mechanism explains the 1/*f* behavior in the applied bias range. Moreover, it is suggested that in order to observe the inter/intra subband scattering impact on the flicker noise much lower applied biases are needed.

II. EXPERIMENTAL

Low frequency noise (LFN) measurements were performed at wafer–level in n-channel GAA NW FETs fabricated at imec on 300 mm wafers. The process description may be found in [5]. Details on the measurement set-up are given in [6].

In order to estimate the low frequency noise parameters, the same methodology as in [1,2,6,7] is applied, assuming that the white noise, flicker noise and generation-recombination noise are non-correlated noise sources. The LF noise is given by the general expression [6]

$$S_{v_g}(f) = B_w + \frac{K_f}{f} + \sum_{i=0}^{N} \frac{A_i}{1+\left(\frac{f}{f_{0i}}\right)^2} \quad (1)$$

where S_{vg} is the input-referred voltage noise, B_w is related to the white noise level, K_f gives the flicker noise level, and the last term of the equation presents a sum of Lorentzian components, with A_i the plateau value and f_{0i} the characteristic frequency. The different parameters can be determined based on a comparison between the experimental data and the model of (1). Typical example of noise parameter estimation is given in Fig. 1.

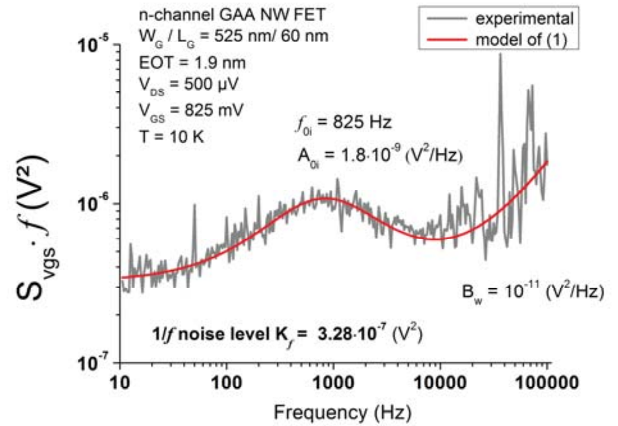

Fig. 1 Typical application of noise parameters estimation.

The LFN study was focused at very low temperature (i.e. 10 K) and was effectuated as a function of the applied gate voltage (V_{GS}) for an applied drain voltage (V_{DS}) of 500 µV and as a function of the applied drain voltage (V_{DS}) for an applied gate voltage (V_{GS}) of 0.5 V.

From Fig. 2, it may be observed that at these polarization conditions, the drain current normalized by the applied drain bias presents step-like effects, leading to oscillations in the transconductance behavior (Fig. 3). For V_{DS} lower than the thermal energy, it may be expected that the drain current and transconductance are not independent on the applied drain voltage in the subthreshold operation. However, the drain current and the transconductance normalized by the applied drain bias not superpose at lower V_{DS} values even in strong inversion regime. This suggests that the step-like effects are related to the subband scattering effects. Using the same procedure as in [8], from the minima of the transconductance oscillations, the subband energy spacing ΔE between the successive energy subband fillings may be estimated. This technique was already successfully applied in UTBOX's, FinFET's and GAA NW FET's [1,2,7]. In our

actual case, the estimated ΔE are between 2 - 7 meV, confirming that the conditions where quantum transport may be observed are fulfilled, i.e., a ΔE higher than the energy induced by the drain voltage (qV_{DS}) and higher than the thermal energy (about 862 μeV at 10 K).

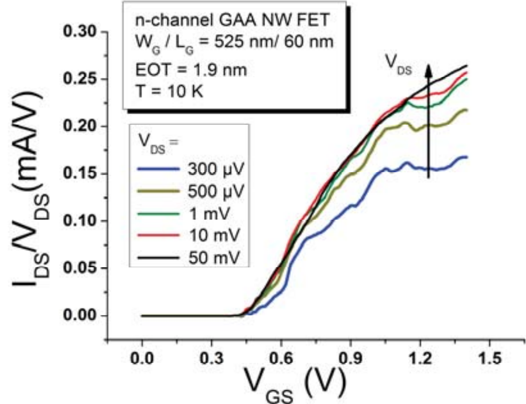

Fig. 2. I_{DS}/V_{DS} characteristics as a function of the applied V_{GS}.

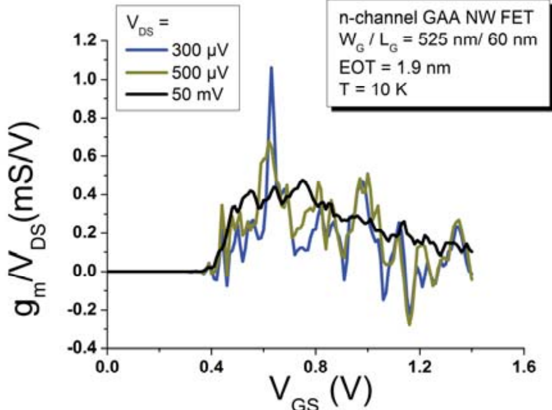

Fig. 3. g_m/V_{DS} characteristics versus V_{GS} .

III. RESULTS

In Fig. 4, the estimated input-referred gate voltage 1/*f* noise levels are plotted as a function of the applied gate voltage at fixed V_{DS} of 500 μV.

Using the methodology presented in [2] the origin of the 1/*f* noise behavior is checked.

As the 1/*f* noise increases with the applied gate voltage, one can use the δn+δμ model described by (13) of [2]. Except for the lowest V_{GS} polarizations a good agreement may be observed between the experimental data and the δn+δμ model, considering a value of the flat-band noise level S_{vfb} of about $1{\cdot}10^{-7}$ V^2/Hz and a c_dn factor of about $3.5{\cdot}V^{-2}$.

However, using a c_dμ factor of $7{\cdot}10^{-7}{\cdot}V$, a good agreement between the data and the δμ model described by (10) of [2] is observed, suggesting that the mobility fluctuations through the Coulomb scattering mechanism may be also responsible for the 1/*f* noise at this applied V_{DS}.

Even if the existence of both δn and δμ fluctuations as independent contributions on the total noise was already evoked [9], it is surprising that both δn+δμ or δμ fluctuation models may explain the flicker noise behavior and this for polarization conditions in which a step-like behavior is observed in the transfer characteristics. One should note that the measured drain current and transconductance read all mobility mechanisms involved in the carrier transport. As the models of (10) or (13) of [2] consider only the Coulomb scattering mechanism (i.e. low vertical electric field), this suggests that even if the inter/intra subband scattering has an important impact on the DC characteristics (see Figs. 1 and 2), for the investigated polarization they do not affect the 1/*f* noise levels.

It may be noticed that the deviation between the data and the δn+δμ or δμ models of [2] at very low applied V_{GS} may be related to the fact that the moderate inversion conditions are not fulfilled.

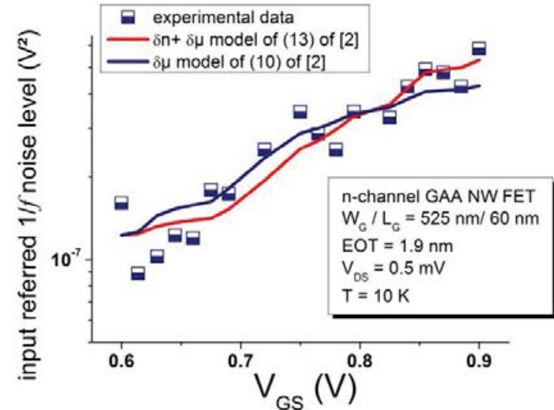

Fig. 4. Input referred 1/*f* noise levels versus V_{GS} at fixed V_{DS} of 500 μV.

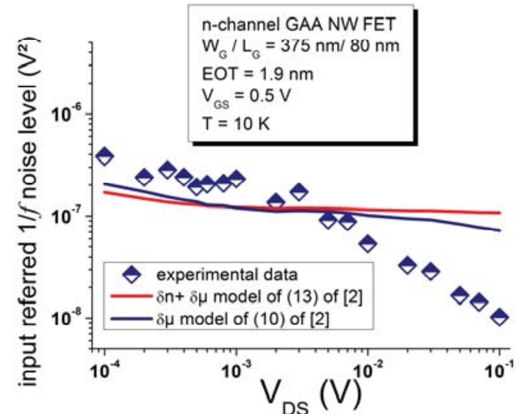

Fig. 5. Input referred 1/*f* noise levels versus V_{DS} at fixed V_{GS} of 0.5 V.

In Fig. 5, the estimated input-referred gate voltage 1/*f* noise levels are plotted as a function of the applied drain voltage at fixed V_{GS} of 0.5 V.

The behavior of the flicker noise levels shows a slight decrease with the increase of V_{DS}, followed by a quick decrease of more than one decade with the further increase of the applied V_{DS} in the range of 1 mV – 100 mV. Assuming the carrier number fluctuation mechanism leads to consider a flat-band noise independent on the applied drain voltage at fixed V_{GS}. This implies that the behavior of the 1/*f* noise levels versus V_{DS} cannot be explained in the framework of the carrier number fluctuation mechanisms. Considering the δn+δμ model, using the same parameters as derived from Fig. 4 (i.e. S_{vfb} of $1{\cdot}10^{-7}$ V^2/Hz and c_dn of $3.5{\cdot}V^{-2}$), it is impossible to fit the experimental data. One should note that in moderate inversion operation, the ratio of the I_{DS}/g_m, which is used in (13) of [2] to model the δn+δμ

mechanism, should increase with the applied V_{DS}, in contradiction with the experimental shape. One can conclude that considering moderate inversion operation, the δn or δn+δμ mechanisms are not responsible for the 1/*f* noise behavior at this temperature and applied polarization.

Moreover, one can observe that using the δμ model described by (10) of [2] cannot explain the 1/*f* noise behavior presented in Fig. 5. Taking into account the quasi-constancy of the I_{DS}/g_m behavior with V_{DS} (see (10) of [2]) it may be suggested that at a V_{GS} of 0.5 V we still operate in weak inversion regime.

A methodology to describe the δn+δμ or δμ models in weak inversion is therefore mandatory.

IV. Theoretical Approach

Taking into account the mobility law for temperatures lower than 40 K (e.g. (3) of [2] derived from [3]), and the expression of the transconductance related to the conductance g_{mG} (e.g. (5) of [2], derived from [9,10]), it may be easily demonstrated that:

- from weak to moderate inversion ($Q_i < Q_m$) the conductance can be expressed as :

$$G_{DS} = 2\frac{W}{L}\frac{\mu_m}{Q_m}Q_i^2 \qquad (2)$$

where L and W are the effective channel length and width, μ_m is the maximum of the effective mobility and Q_m is the corresponding inversion charge density; Q_i being the inversion charge density at arbitrary V_{GS}.

- while in weak inversion ($Q_i < Q_m$ and $C_i << C_d$, C_{ss}, C_{ox}, where C_i, C_d, C_{ss} and C_{ox} are the inversion, the depletion, the interface state and the gate oxide capacitances per unit of area, respectively), the transconductance related to the conductance g_{mG} will read:

$$g_{mG} = \left(4\frac{W}{L}C_i\frac{\mu_m}{Q_m}\right)\cdot Q_i = \left(4\frac{W}{L}\frac{q}{k_BT}\frac{\mu_m}{Q_m}\right)\cdot Q_i^2 \qquad (3)$$

Using the same methodology as in [2], the resulting expressions for the δn+δμ [11] or δμ [12] models may be finally derived as in Table 1:

Table 1

Summary of δμ and δn+δμ models as a function of G_{DS} and g_{mG}

	weak inversion	moderate inversion
δμ	$S_{v_{gs}} = \frac{c1_d\mu}{fLW}\frac{I_{DS}^2}{g_m^2}\frac{1}{\sqrt{g_{mG}}}$ (a)	$S_{v_{gs}} = \frac{c_d\mu}{f}\frac{I_{DS}}{g_m}$ (derived from (10) of [2]) $S_{v_{gs}} = \frac{c2_d\mu}{fLW}\frac{I_{DS}^2}{g_m^2 g_{mG}}$ (b)
	$S_{v_{gs}} = \frac{c3_d\mu}{fLW}\frac{I_{DS}^2}{g_m^2}\frac{1}{\sqrt{G_{DS}}}$ (c)	
δn+δμ	$S_{v_{gs}} = S_{v_{FB}}\left[1+c1_dn\left(\frac{I_D}{g_m}\right)\sqrt{g_{mG}}\right]^2$ (d)	$S_{v_{gs}} = S_{v_{FB}}\left[1+c_dn\left(\frac{I_D}{g_m}\right)\right]^2$ (derived from (13) of [2]
	$S_{v_{gs}} = S_{v_{FB}}\left[1+c2_dn\left(\frac{I_D}{g_m}\right)\sqrt{G_{DS}}\right]^2$ (e)	

where the different coefficients are summarized in Table 2:

Table 2

Summary of coefficients used in the equations presented in Table 1

$c1_d\mu = \alpha_H q\sqrt{4\frac{W}{L}\frac{q}{k_BT}\frac{\mu_m}{Q_m}}$	(a)
$\frac{c1_d\mu}{c3_d\mu} = \sqrt{2\frac{q}{k_BT}}$	(b)
$c2_d\mu = \alpha_H q 4C_{ox}\frac{W}{L}\frac{\mu_m}{Q_m}$	(c)
$c1_dn = \alpha_H q\sqrt{4\frac{W}{L}\frac{k_BT}{q}\frac{\mu_m}{Q_m}}$	(d)
$\frac{c1_dn}{c2_dn} = \sqrt{\frac{q}{2k_BT}}$	(e)

where k_B is the Boltzmann constant and q is the elementary charge.

Assuming as usual that the inversion charge from weak to moderate inversion presents an exponential dependency with the applied drain bias, the equations presented in Table 1 becomes:

Table 3

Summary of δμ and δn+δμ models as a function of I_{DS} and g_m

	weak inversion	moderate inversion
δμ	$S_{v_{gs}} = \frac{c4_d\mu}{f}\frac{I_{DS}^2}{g_m^{5/2}}$ (a)	$S_{v_{gs}} = \frac{c_d\mu}{f}\frac{I_{DS}}{g_m}$ (derived from (10) of [2] $S_{v_{gs}} = \frac{c5_d\mu}{f}\frac{I_{DS}^2}{g_m^3}$ (b)
	$S_{v_{gs}} = \frac{c6_d\mu}{f}\frac{I_{DS}^{3/2}}{g_m^2}$ (c)	
δn+δμ	$S_{v_{gs}} = S_{v_{FB}}\left[1+c3_dn\left(\frac{I_D}{g_m^{1/2}}\right)\right]^2$ (d)	$S_{v_{gs}} = S_{v_{FB}}\left[1+c_dn\left(\frac{I_D}{g_m}\right)^2\right]^2$ (derived from (13) of [2]
	$S_{v_{gs}} = S_{v_{FB}}\left[1+c4_dn\left(\frac{I_D^{3/2}}{g_m}\right)\right]^2$ (e)	

where c4_dμ, c5_dμ and c6_dμ are related to c1_dμ, c2_dμ and c3_dn; c3_dn and c4_dn are related to c1_dn and c2_dn with the respect of the integration coefficient of the inversion charge with the drain bias.

V. Discussion

Assuming the weak inversion operation mode, the δn+δμ model will be described by Eq. (d) or (e) presented in Table 3. Taking into account the experimental quasi-independence (in agreement with the expected theoretical independence) of the I_{DS}/g_m behavior with V_{DS} observed in Fig. 5, it is obvious that the δn+δμ model will provide 1/*f* noise levels which will increase with the increase of V_{DS}, in contradiction with the experimental behavior presented in Fig. 5.

It should be noted that the c_dn factor of about $3.5\cdot V^{-2}$

(used to model results presented in Fig 4 in the framework of the δn+δμ model) lead to a Coulomb scattering coefficient (α_C) value of about $0.02 \cdot 10^4$ Vs/C. Taking into account the generally reported value of α_C in the range of $1 \cdot 10^4$ Vs/C [11] this obtained value may be considered as an unphysical one.

All these arguments demonstrate that the hypothesis of the δn or δn+δμ fluctuation mechanism in order to explain the flicker noise behavior can be completely dismissed.

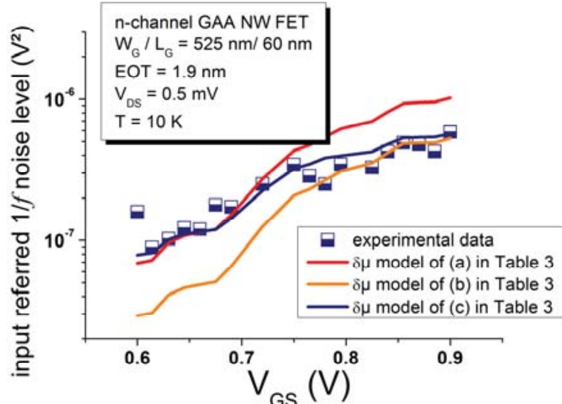

Fig. 6. Input referred 1/*f* noise levels versus V_{GS} at fixed V_{DS} of 500 μV.

Eq. (c) of Table 3 permits to model correctly the experimental 1/*f* noise behavior and this from weak to moderate inversion operation as observed in Fig. 6. This confirms our hypothesis: the mobility fluctuations through the Coulomb scattering mechanism are responsible for the 1/*f* noise behavior versus V_{GS}.

Applying Eq. (a) of Table 3 permits to obtain a good agreement between the model and data in weak inversion; the same result is obtained using Eq. (b) in moderate inversion. Employing Eq. (a) and (b) of Table 3 permits to identify the different operation modes at V_{DS} = 500 μV: weak inversion till around an applied V_{GS} of about 0.7 V and moderate inversion for V_{GS} higher than about 0.75 V.

The first experimental point (at V_{GS} = 0.6 V) cannot be modelled employing the equations of Table 3, suggesting that for much lower polarization than studied, the inter/intra subband scattering will impact the flicker noise levels.

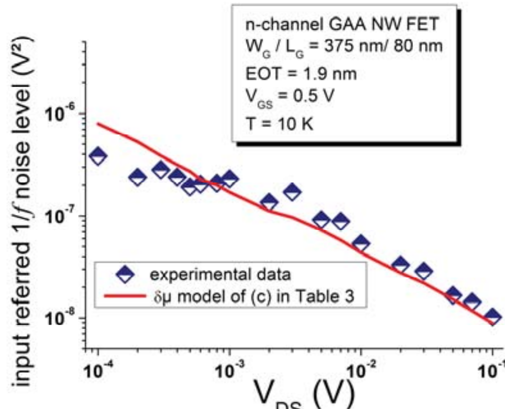

Fig. 7. Input referred 1/*f* noise levels versus V_{DS} at fixed V_{GS} of 0.5 V.

Taking into account the same value of the coefficient c6_dμ as for Fig. 6, one can observe that the δμ model provides some trend for the flicker noise behavior as a function of V_{DS} for V_{DS} higher than 1 mV (Fig. 7). This corroborates with the hypothesis that Coulomb scattering mechanisms are responsible for the 1/*f* noise fluctuations.

However, a new physical model is necessary to clearly state the drain current evolution with V_{DS} in order to explain the flicker noise behavior as a function of the applied V_{DS}, in particular at the lowest applied V_{DS}.

VI. Conclusion

It was clearly demonstrated that the carrier number or carrier number correlated to mobility fluctuations mechanism cannot explain conveniently the flicker noise behavior.

Even if the inter/intra subband scattering affect the DC measurements, there is a polarization interval in which they do not impact the 1/*f* noise. It was proved that in this low polarization range, the Coulomb scattering mechanism is responsible for the 1/*f* noise fluctuations.

References

[1] D. Boudier, B. Cretu, E. Simoen, A. Veloso, and N. Collaert, "Discussion on the 1/f noise behavior in Si gate-all-around nanowire MOSFETs at liquid helium temperatures," In Proc. 2018 Joint International EUROSOI Workshop and International Conference on Ultimate Integration on Silicon (EUROSOI-ULIS), pp. 1-4, 2018, DOI: 10.1109/ULIS.2018.8354739

[2] B. Nafaa, B. Cretu, N. Ismail, O. Touayar, R. Carin, E. Simoen, and A. Veloso, "Low-frequency noise measurements at liquid helium temperature operation in ultra-thin buried oxide transistors – Physical interpretation of transport phenomena," *Solid-State Electron.*, vol. 150, pp. 1-7, 2018, DOI: 10.1016/j.sse.2018.08.010.

[3] G. Ghibaudo and F. Balestra, "Modelling of ohmic MOSFET operation at very low temperature," *Solid-State Electron.*, vol. 31, no. 1, pp. 105-108, 1988, DOI: 10.1016/0038-1101(88)90092-5.

[4] D. Jeon and D. Burk, "MOSFET electron inversion layer mobilities-A physically based semi-empirical model for a wide temperature range," *IEEE Trans. Electron Dev.*, vol. ED - 36, no.2, pp. 1456-1463, 1989, DOI: 10.1109/16.30959.

[5] A. Veloso, M.J. Cho, E. Simoen, G. Hellings, P. Matagne, N Colaert, and A. Thean, "Gate-all-around nanowire FETs vs. triple-gate FinFETs: on gate integrity and device characteristics," *ECS Trans.*, vol. 72 (2), pp. 85-95, 2016, DOI: 10.1149/07202.0085ecst.

[6] D. Boudier, B. Cretu, E. Simoen, R. Carin, A. Veloso, N. Collaert, and A. Thean, "Low frequency noise assessment in n- and p-channel sub-10 nm triple-gate FinFETs: Part I: Theory and methodology," *Solid-State Electron.*, vol. 128, pp. 102-108, 2017, DOI: 10.1016/j.sse.2016.10.012.

[7] D. Boudier, B. Cretu, E. Simoen, A. Veloso, and N. Collaert, "Detailed characterisation of Si Gate-All-Around Nanowire MOSFETs at cryogenic temperatures," *Solid-State Electron.*, vol. 143, pp. 27-32, 2018, DOI: 10.1016/j.sse.2018.02.015

[8] K. Morimoto, Y. Hirai, K. Yuki, and K. Morita, "Fabrication and transport properties of silicon quantum wire gate-all-around transistor," *Jpn. J. Appl. Phys.*, vol. 35, pp. 853-857, 1996, DOI: 10.1143/JJAP.35.853

[9] G. Ghibaudo, "Analytical modelling of the MOS transistor," *Phys. Stat. Sol. (a)*, vol. 113, no. 1, pp. 223-240, 1989, DOI: 10.1002/pssa.2211130127

[10] G. Ghibaudo, "An analytical model of conductance and transconductance for enhanced-mode MOSFETs," *Phys. Stat. Sol.* (a) 1986;96:323–35. https://doi.org/10.1002/pssa.2210950141.

[11] G. Ghibaudo, O. Roux, Ch. Nguyen-Duc, F. Balestra, J. Brini, "Improved analysis of low frequency noise in field-effect MOS transistors," *Phys. Stat. Sol.* (a), 124, 571, 1991, DOI: 10.1002/pssa.2211240225.

[12] F. Hooge, "1/f is no surface effect," *Phys. Lett. A*, vol. 29, no. 3, pp. 139-140, April 1969, DOI: 10.1016/0375-9601(69)90076-0.